ONIOM Calculation on Azurin: Effect of Metal Ion Substitutions

V. Rajapandian, V. Hakkim, and V. Subramanian*

Chemical Laboratory, Central Leather Research Institute, Council of Scientific and Industrial Research, Adyar, Chennai 600 020, India

Received: January 15, 2009; Revised Manuscript Received: May 16, 2009

In this study an attempt has been made to investigate the effect of metal ion substitution on the structure and spectra of azurin using two-layer ONIOM (our own *N*-layered integrated molecular orbital + molecular mechanics) approach. It is evident from the results that the overall structure of the protein is not altered by metal ion substitution; nevertheless, the metal ion binding site undergoes noticeable changes. The present study highlights the importance of protein milieu in the prediction of structure, electronic, and spectral properties of native and substituted azurins and illustrates the usefulness of ONIOM approach in the designing and engineering of metalloproteins.

Introduction

Studies on metalloproteins have attracted considerable interest among many researchers owing to their biological functions.[1] Particularly copper-containing metalloproteins have received intensive attention due to its coordination environment, redox, and spectroscopic properties of copper as well as the surrounding protein milieu.[2,3] Among the copper proteins, numerous studies have been carried out on "blue copper protein" such as plastocyanin and azurin.[4,5] Azurin from *Pseudomonas aeruginosa* (Pa) is a small blue copper protein with type-I copper site and it belongs to the family of cupredoxins. It is involved in the transport of electrons from the membrane bound complex to a soluble nitrite reductase (cd_1) in the periplasmic space of the bacterium.[6,7] The X-ray structural studies have revealed that azurin consists of a single copper ion bound to a polypeptide chain of 128 amino acid residues. The secondary structural organization of azurin has been characterized as a single short α-helix, eight β-strands, and two β-sheets folded into a Greek-key motif.[8]

The schematic representation of the azurin active site is shown in Figure 1. In the active site of azurin, the copper ion is covalently bonded to thiolate group of cystine (S^{γ}(C112)) and coordinated with nitrogen atoms of two histidine residues ($N^{\delta 1}$(H46) and $N^{\delta 1}$(H117)) in a trigonal planar conformation. The thioether group of the methionine (S^{δ}(M121)) serves as an axial ligand, resulting in a trigonal pyramidal coordination geometry around the copper ion. A second axial group, the backbone amide oxygen of the glycine (O(G45)), electrostatically interacts with the copper ion resulting in distorted trigonal bipyramidal (TBP) geometry around the metal ion coordination site. The blue copper proteins exhibit three properties that differ from what are found in the small inorganic copper complexes: a strong absorption around 600 nm, small narrow hyperfine coupling constants in the electron spin resonance spectrum, and a high-reduction potential.[1,8,9]

Many groups have investigated the structure−function relationship of blue copper proteins using both experimental and theoretical methods.[2−7] Solomon et al. have made seminal contributions to the understanding of the structure, spectra, and functional properties of these copper proteins.[5b,10] They have employed different spectroscopic techniques combined with high-quality electronic structure calculations to explore the structure, spectra, and reactivity of blue copper proteins. The active site geometries obtained from X-ray diffraction studies have been used to predict the spectra and redox properties.

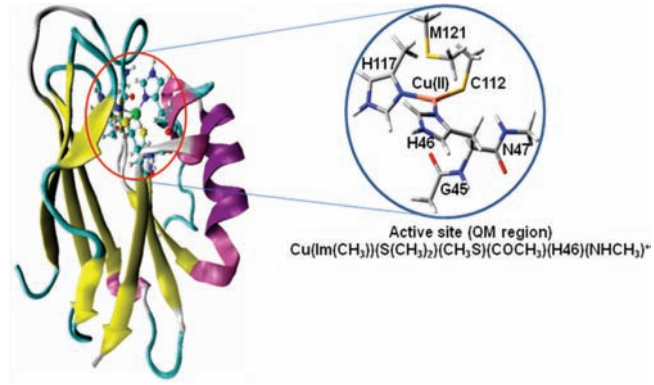

Figure 1. Coordination sphere model (QM region) shown to the right. The rest of the protein parts are considered as MM part.

During the last decades, numerous electronic structure calculations have been carried out on the blue copper proteins using cluster models.[11,12] Ryde et al. have performed extensive studies on small model systems of the active site of type-I copper sites.[13] They found an active site geometry that is remarkably similar to the ones observed in plastocyanin, a typical type-I copper protein that lacks the axial glycine residue observed in azurin. Many studies have been undertaken to model the effect of metal ion substitutions and mutation of amino acids in the coordination environment.[1a,2,14,15] De Kerpel et al. have reported problems in the prediction of active site geometries in the case of native and substituted azurins.[16] It has also shown in different studies that distal mutation does not have any influence on the structure and properties of azurin.[1a,2,14,15] Previous experimental studies on Co(II), Ni(II), and Zn(II) substituted azurins revealed the structural changes in the metal ion binding site.[17] Due to these substitutions, the geometry of the metal site varies from distorted TBP to distorted tetrahedral (T_d) leads to changes in the activity.[18] Crystal structures and NMR spectroscopy have indicated the carbonyl oxygen (O(G45)) binds much more

* To whom correspondence should be addressed. Tel.: +91 44 24411630. Fax: +91 44 24911589. E-mail: subuchem@hotmail.com, subbu@clri.res.in.

10.1021/jp900451f CCC: $40.75
Published on Web 07/02/2009

strongly in the Co(II), Ni(II), and Zn(II) substituted azurins than in the native protein.[17−19] Thus, these metal ion substituted azurin sites adopt a distorted T_d geometry where the metal ion moves closer to oxygen of the backbone carbonyl oxygen (O(G45)) and simultaneously away from the axial S^{δ}(M121) residue.

Several studies have been made in the past to predict the d−d, ligand-to-metal, and metal-to-ligand charge transfer transitions using experimental and theoretical methods.[1a,2,10,13,20,23b] Both "active site only" models and spectroscopically parametrized density functional theory (DFT) calculations has been used to predict the properties of blue copper proteins. Swart et al. have made significant contributions to the understanding of azurin using hybrid quantum mechanics/molecular mechanics (QM/MM) calculations.[2,21] In QM/MM calculations, the active site region was treated at QM and the remaining protein along with the solvent molecule was treated as MM.[2,21] It is found that the calculated geometrical parameters are in good agreement with the X-ray diffraction results. In the same study, the excitation energies have been calculated using semiempirical (CNDO/INDO) methods and the surrounding protein and solvent environment were considered with a polarizable classical force field. It is observed that calculated excitation energies are in good agreement with the experimental results. Roethlisberger et al. have carried out a study of the electronic structure and excitation spectra of the oxidized form of the azurin using hybrid QM/MM with time-dependent density functional theory[22] (TDDFT).[23] In the previous study, it was shown that inclusion of backbone hydrogen bonding interaction ((C112)$S^{\gamma}\cdots$N(N47)) is necessary to obtain convergence and reliable estimates of excitation energies.[2,23b] In the present study the QM region was truncated to include the backbone group ($-NHCH_3$) of N47 residue.

In the prediction of structure and reactivity of metalloproteins, both "active site only" models and the complete structure of the metalloproteins have been used. The "active site only" models are treated using QM methods whereas the full metalloprotein is probed using QM/MM or ONIOM approaches. Siegbahn et al. have demonstrated the usefulness of "active site only" models in the prediction of structure and reactivity of metalloproteins.[24]

In addition, studies on different blue copper proteins reveal that the electrostatic field produced by the protein framework directly influences the redox properties.[2,21,23] Rothlisberger and co-workers have shown that the importance of protein field in the calculation of optical absorption.[23] They have reported the changes in the Kohn−Sham orbital energies, and as a consequence red shifts are observed in the low-energy and high-energy bands as well as blue shift in the central band. They have related these shifts to the electrostatic field anisotropy along the z-axis in the binding site produced by the α-helix, which is at 9 Å from the copper center.

In this study, a systematic work has been carried out to investigate the effect of metal ion substitutions on the structure and spectroscopic properties of azurin with complete protein environment using ONIOM approach. Specifically, the effect of substitution on Cu(II)−azurin by Co(II), Ni(II), and Zn(II) has been addressed in this study. Both ligand field (LF) and ligand to metal charge transfer (LMCT) transitions have been calculated using the TDDFT method combined with the ONIOM approach. A detailed comparison has also been made with previous experimental and theoretical investigations.

Computational Details

The usefulness of ONIOM (MO:MO) and ONIOM (MO:MM) strategies to explore complex questions in large systems has been demonstrated.[25,26] In this study, we have performed ONIOM calculations on the native and substituted azurins to predict the electronic structure and spectra. The experimental X-ray structure of azurin from Pa was retrieved from the Brookhaven Protein Databank (PDB ID: 4AZU).[8] Charges of amino acids were treated appropriately: glutamate and aspartate residues were assigned as negative, while lysine, and arginine residues were assigned as positive. All the $N^{\varepsilon 2}$(H) positions were protonated. The deprotonated model of C112 residue was used in all the calculations. The ONIOM model consists of 1927 atoms, with 56 active site atoms in the QM region and the remaining atoms in the MM region.

The active site of azurin was modeled by including complete protein environment using the two-layer ONIOM (QM:MM) method (Figure 1). Spin unrestricted DFT with Becke's[27] three-parameter hybrid exchange functional and the Lee−Yang−Parr[28] correlation functional DFT (B3LYP) were used for the active site and the remaining protein part was treated using universal force field[29] (UFF). DFT (B3LYP) optimization calculations were performed using 6-31G* and 6-311G** basis sets.[30] The complete geometries of native and metal-substituted azurin were optimized using the ONIOM approach. This optimized geometries from 6-31G* were used for the prediction of spectroscopic properties using TDDFT (B3LYP) employing TZVP, 6-311+G*, and 6-311+G** basis sets. The optimized QM region was extracted from ONIOM (QM:MM) optimized geometry. The single point calculations were performed for the QM regions to compute partial charges, spin densities, and molecular orbital compositions using Mulliken population analysis (MPA), natural population analysis (NPA), and molecular orbital coefficients in the natural atomic orbital (NAOMO) schemes.[31] All these calculation were carried out using Gaussian 03 program package (Revision E.01).[32] The native, Co(II)-, Ni(II)-, and Zn(II)-substituted azurins are designated as Cu(II)−Az, Co(II)−Az, Ni(II)−Az, and Zn(II)−Az in the remaining part of the text.

Results and Discussion

Importance of Protein Environment. With a view to assess the importance of protein environment on the geometrical parameters, the "active site models" of Cu(II)−Az, Co(II)−Az, Ni(II)−Az, and Zn(II)−Az were optimized without any geometrical constraints at the B3LYP/6-31G* level. The optimized geometries for different azurin models are presented in Figure 2. It can be seen that axial ligand distances corresponding to M121 and G45 residues are 3.476 and 3.604 Å for Cu(II)−Az. The corresponding distances from an X-ray diffraction study are 3.149 ± 0.070 and 2.967 ± 0.093 Å, respectively.[2] The axial ligand distances in the "active site only" models are overestimated due to absence of a protein environment. A similar problem has been encountered with the prediction of axial ligand distances in the "active site only" models of substituted azurins. In addition, the M121 residue moves completely away and forms H-bond with the $H^{\varepsilon 2}$ of H46 residue in the substituted azurins due to a shallow potential energy surface.[2,16] Further "active site only" modeling yields much larger root-mean-square deviation (rmsd) with reference to the geometrical parameters obtained from the X-ray structure, which indicates the importance of the complete protein environment in the prediction of structure and properties of metalloproteins. Hence, all calculations have been carried including protein environment using the ONIOM approach.

Active Site Geometry. Among the different blue copper proteins, the coordination number of the azurin is 5. The backbone carbonyl oxygen of G45 in the axial position

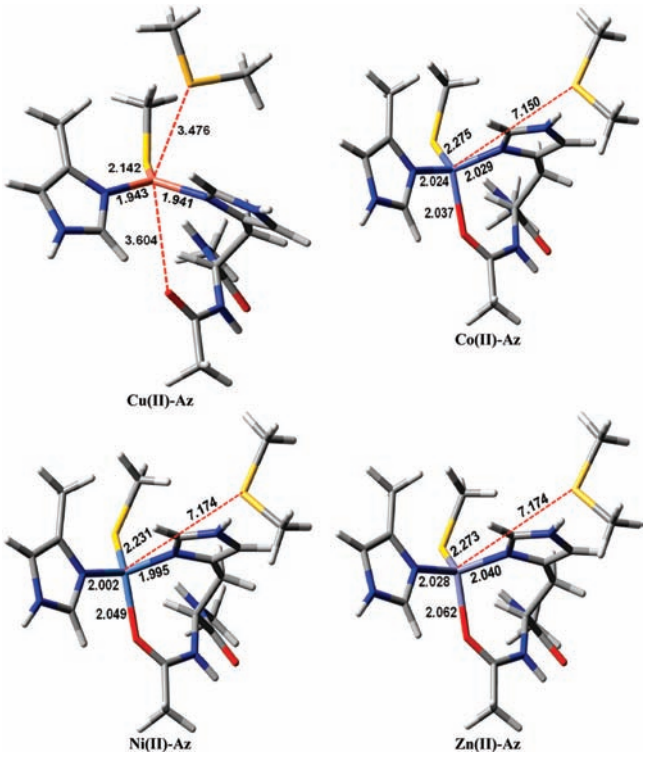

Figure 2. Active site only models of native and substituted azurins were optimized using B3LYP/6-31G* level.

Coulombically interacts with the Cu(II) ion. Although, this axial interaction plays a superfluous role,[17b] It differentiates azurin from the other blue copper proteins. The calculated geometrical parameters for the native and substituted azurins are presented in Tables 1 and 2 along with experimental and computationally predicted values. The active site geometries of substituted azurins are also shown in Figure 3. Table 3 shows the distance of metal ion from the plane of coordination comprising of (H46)$N^{\delta 1}$−(H117)$N^{\delta 1}$−(C112)S^{γ} atoms. It is clearly evident that native Cu(II)−Az has distorted TBP geometry in accordance with the X-ray diffraction and other experimental studies.[17,18]

The active site and immediate protein environment undergo noticeable changes upon binding with Co(II), Ni(II), and Zn(II). It is found that the five coordination environment in native protein changes to four coordinate arrangements in the substituted azurin in accordance with the previous reports. It can adopt any four coordination geometry with point group symmetry, viz., T_d, D_{4h}, C_{4v}, and C_{2v}. In this context, it is worth analyzing the inherent tendencies of Co(II), Ni(II), and Zn(II) ions to form various coordination environments.

The number of inorganic and organometallic compounds of Co(II) in various stereochemical types have been reported.[33] Octahedral and tetrahedral arrangements are the most common types. However, reasonable numbers of four and five coordinate complexes are reported in the literature.[33] It is found from the chemistry of Co(II) complexes that it readily forms tetrahedral

TABLE 1: The Calculated Bond Distances[d] of the Native and Substituted Azurins (Å)

	M(II)−S^{γ}(C112)	M(II)−$N^{\delta 1}$(H46)	M(II)−$N^{\delta 1}$(H117)	M(II)−-S^{δ}(M121)	M(II)−O(G45)
X-ray structure of Cu(II)−Az[a]	2.237 ± 0.044	2.076 ± 0.060	2.011 ± 0.069	3.149 ± 0.070	2.967 ± 0.093
Solomon et al.[b]	2.21	2.06	2.03	3.06	2.68
Swart et al.[a]	2.169	2.017	1.995	3.178	2.855
Rothilsberger et al.[c]	2.13 ± 0.04	1.98 ± 0.06	1.99 ± 0.05	3.32 ± 0.28	3.20 ± 0.22
Cu((II)−Az[d]	2.140	1.956	1.945	3.356	2.947
X-ray structure of Co(II)−Az[a]	2.337 ± 0.024	2.243 ± 0.045	2.421 ± 0.099	3.561 ± 0.126	2.230 ± 0.077
Swart et al.[a]	2.196	2.038	2.013	3.552	2.089
Co(II)−Az[d]	2.239	2.075	2.035	3.631	2.074
X-ray structure of Ni(II)−Az[a]	2.39 ± 0.07	2.23 ± 0.09	2.22 ± 0.12	3.30 ± 0.05	2.46 ± 0.06
Swart et al.[a]	2.172	2.059	2.055	3.209	2.123
Ni(II)−Az[d]	2.228	2.032	2.011	3.707	2.058
X-ray structure of Zn(II)−Az[a]	2.300 ± 0.022	2.069 ± 0.050	2.007 ± 0.036	3.384 ± 0.094	2.139 ± 0.091
Swart et al.[a]	2.240	2.085	2.056	3.484	2.173
Zn(II)−Az[d]	2.255	2.066	2.018	3.859	2.100

[a] Hybrid QM/MM calculations. Taken from ref 2. [b] The active site of the azurin was optimized, keeping the backbone C and N atom coordinates constrained to their crystallographic positions. From ref 10g. [c] Hybrid quantum mechanics/ molecular dynamics calculation. From ref 23b. [d] Present study.

TABLE 2: Calculated Bond Angles (deg)

	S^{γ}(C112)− M(II)− $N^{\delta 1}$(H46)	S^{γ}(C112)− M(II)− $N^{\delta 1}$(H117)	S^{γ}(C112)− M(II)− O(G45)	S^{γ}(C112)− M(II)− S^{δ}(M121)	$N^{\delta 1}$(H46)− M(II)− $N^{\delta 1}$(H117)	$N^{\delta 1}$(H46)− M(II− O(G45)	$N^{\delta 1}$(H46)− M(II)− S^{δ}(M121)	$N^{\delta 1}$(H117)− M(II)− O(G45)	$N^{\delta 1}$(H117)− M(II)− S^{δ}(M121)	S^{δ}(M121)− M(II)− O(G45)
X-ray structure of Cu(II)−Az[a]	130	122	100	110	107	81	69	92	84	147
Swart et al.[a]	130	127	94	111	102			85		151
Cu(II)−Az[b]	131	126	108	102	103	72	74	81	95	145
X-ray structure of Co(II)−Az[a]	129	122	104	104	107	73	75	107	73	147
Co(II)−Az[b]	127	116	106	95	113	87	71	94	85	156
X-ray structure of Ni(II)-Az[a]	113	119	101	99	120	87	64	108	82	149
Ni(II)-Az[b]	130	125	104	97	103	88	71	90	85	157
X-ray structure of Zn(II)-Az[a]	122	119	102	103	105	83	67	103	82	148
Zn(II)-Az[b]	129	121	105	100	107	87	66	93	84	152

[a] Hybrid QM/MM calculations. Taken from ref 2. [b] Parameters of the native and substituted azurins.

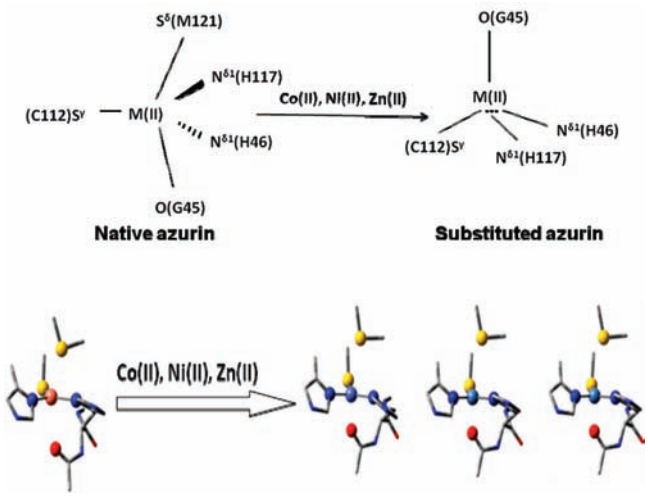

Figure 3. The optimized active site geometries of Cu(II)−Az and substituted azurins.

complexes when compared to other metal ions. Several inorganic and organometallic compounds of Ni(II) have been reported in the literature.[34] It can assume four, five, and six coordination environments and all the other main structural types. When small substituents are present, Ni(II) prefers to form planar or nearly planar complexes. Regular tetrahedral complexes are rarely found in Ni(II) except for the NiX_4^{2-}.[17c,34] In general, Zn(II) can be found in small molecule structures with a variety of coordination numbers from two to eight.[35] Since, there is no LF stabilization effect in the Zn(II) ion due to completed d (d^{10}) shell, its stereochemistry is determined by consideration of size, electrostatic, and covalent binding forces.[17c,35] In most cases, the Zn(II) tends to adopt four coordination environment. This analysis shows that substituted azurins can form any one of the four coordination environments. However, the calculated geometrical parameters reveal that Co(II)−Az, Ni(II)−Az, and Zn(II)−Az adopts distorted tetrahedral arrangement due to inherent tendencies of the metal ions and protein environment.

It can be found from Table 1 that M(II)−S^{γ}(C112), M(II)−$N^{\delta1}$(H46), M(II)−$N^{\delta1}$(H117), M(II)−S^{δ}(M121), and M(II)−O(G45) distances are in good agreement with the X-ray structures[2,17,18] and theoretically predicted values.[2,10g,23b] In substituted azurin, M(II)−L distances are longer except for the backbone oxygen ligand, which is shorter by 0.8 Å. As a result, M(II) ion moves in the direction of the G45 backbone oxygen atom. Ni(II)−Az coordinates more strongly with the carbonyl oxygen of O(G45) as a result Ni(II)−S^{δ}(M121) increases by 3.707 Å. Substitution of Cu(II) by Co(II), Ni(II), and Zn(II) leads to a loss of covalency of M(II)−S^{δ}(M121) bond and as a consequence the electrostatic interaction between the metal ion and O(G45) increases. It can be noted from the results that the deviations in M(II)−L distances are within experimental error.

It is evident from the Table 2 that the calculated Ligand−M(II)−Ligand (L−M(II)−L) angles are in reasonable agreement with X-ray structure and other values reported in the earlier studies.[2,17,18] A systematic comparison of bond angles obtained from ONIOM calculation with X-ray diffraction values reveals that the percentage of error in the bond angle ranges from 0.77 to 11.96, 1.55 to 12.15, 1.49 to 16.67, and 1.49 to 9.71 for Cu(II)−Az, Co(II)−Az, Ni(II)−Az, and Zn(II)−Az, respectively. It is worth mentioning that the active site of Ni(II)−Az is intermediate between those of Cu(II)−Az and Zn(II)−Az which is in good agreement with the previous experimental results.[17b] It can be seen from Table 3 that the axial distances of metal ions Co(II), Ni(II), and Zn(II) with respect to the center of the coordination plane lie below the plane by 0.24, 0.20, and 0.22 Å, respectively.

Electronic Structure. Since the entire protein environment is included in the ONIOM calculation, the point group of the native and substituted azurin is C_1. All molecular orbitals of the systems have *A* symmetry. The native azurin consists of 122α and 121β electrons. The singly occupied molecular orbital (SOMO) is 122β, which is involved in the electron transfer and is similar to the lowest unoccupied molecular orbital (LUMO). Energies of β spin orbitals and the molecular orbital compositions of native azurin obtained from NAOMO analysis using B3LYP/TZVP method are presented in Table 4. Co(II)−Az has

TABLE 3: Axial Distance of Metal Ion from the Plane Constituted by the S^{γ}(C112), $N^{\delta1}$(H46), and $N^{\delta1}$(H117) Atoms (Å)

M(II)−($N^{\delta1}N^{\delta1}S^{\gamma}$) distance	Cu(II)−Az	Co(II)−Az	Ni(II)−Az	Zn(II)−Az
X-ray structure[a]	0.083 ± 0.051	0.207 ± 0.071	0.18	0.164 ± 0.042
Swart et al.[a]	0.094	0.230	0.082	0.158
calcd distance in the present study	0.108	0.238	0.202	0.215

[a] Hybrid QM/MM calculations. Taken from ref 2.

TABLE 4: Molecular Orbital Descriptions from Population and NAOMO Coefficient Analysis of β-Spin Orbitals of Cu(II)−Az

			Cu(II)[b]		S^{γ}(C112)[b]		$N^{\delta1}$(H46)[b]		$N^{\delta1}$(H117)[b]		S^{δ}(M121)[b]		O(G45)[b]	
orbital level[a]	energy (eV)[a]	occ[a]	3d	4s	3s	3p	2s	2p	2s	2p	3s	3p	2s	2p
122a	−0.24612	0	39.46	0.00	0.00	44.77	1.09	3.24	1.22	3.76	0.00	0.01	0.00	0.02
121a	−0.32502	1	1.55	0.01	0.00	2.90	0.03	0.20	0.00	0.01	0.00	80.97	0.00	0.16
120a	−0.34497	1	0.89	0.16	0.05	4.38	0.01	0.23	0.02	0.16	0.01	0.11	0.00	6.59
119a	−0.34574	1	3.04	0.07	0.02	4.04	0.01	0.23	0.14	0.60	0.00	0.22	0.00	0.64
118a	−0.35213	1	4.04	0.07	0.06	6.85	0.05	0.57	0.18	1.59	0.03	0.05	0.01	1.38
117a	−0.35450	1	11.81	1.50	0.28	39.80	0.02	0.28	0.47	2.52	0.04	3.79	0.00	2.94
116a	−0.36131	1	8.73	0.52	0.07	17.37	0.12	0.80	0.12	0.80	0.07	0.14	0.01	29.08
115a	−0.36200	1	17.53	0.25	0.01	29.02	0.87	3.62	0.14	1.30	0.01	0.03	0.00	15.72
114a	−0.36739	1	1.65	0.07	0.09	3.53	0.07	1.13	0.09	0.56	0.09	0.56	0.00	23.52
113a	−0.37333	1	2.52	0.00	0.09	0.64	0.06	1.59	0.05	0.28	0.16	0.36	0.00	25.90
112a	−0.40179	1	39.62	0.83	0.88	3.70	0.29	2.94	0.29	15.42	1.70	6.60	0.06	1.81
111a	−0.40625	1	39.72	0.83	0.94	3.23	0.17	1.99	0.10	12.00	2.75	11.51	0.02	1.44
110a	−0.41447	1	54.54	0.04	0.12	1.78	0.03	15.78	0.06	0.42	0.41	2.10	0.03	0.50

[a] Occupation (occ) and MO energies were taken from population analysis. [b] MO coefficients in the natural atomic orbital (NAOMO) analysis.

TABLE 5: Molecular Orbital Descriptions from Population and NAOMO Coefficient Analysis of β-Spin Orbitals of Co(II)−Az

			Co(II)[b]		S^{γ}(C112)[b]		$N^{\delta1}$(H46)[b]		$N^{\delta1}$(H117)[b]		S^{δ}(M121)[b]		O(G45)[b]	
orbital level[a]	energy (eV)[a]	occ[a]	3d	4s	3s	3p	2s	2p	2s	2p	3s	3p	2s	2p
122a	−0.1508	0	73.30	2.17	0.18	0.10	0.07	1.18	0.06	0.98	0.31	0.72	0.55	1.33
121a	−0.1631	0	74.72	0.00	0.05	11.20	0.36	1.43	0.72	2.18	0.01	0.00	0.01	0.10
120a	−0.1779	0	73.04	0.86	0.04	9.01	0.20	0.37	0.08	0.37	0.02	0.07	0.00	0.39
119a	−0.3096	1	14.69	0.02	0.01	72.23	0.01	0.11	0.00	0.10	0.00	0.10	0.02	0.19
118a	−0.3181	1	0.81	0.03	0.02	0.87	0.00	0.02	0.00	0.01	0.00	84.76	0.00	0.02
117a	−0.3391	1	20.30	0.89	3.43	56.93	0.02	0.02	0.04	0.28	0.04	0.69	0.00	0.09
116a	−0.3487	1	0.73	0.06	0.07	3.23	0.00	0.04	0.00	0.01	0.00	0.02	0.00	0.65
115a	−0.3506	1	37.68	0.13	0.05	3.54	0.01	0.05	0.00	1.79	0.01	0.55	0.02	0.92
114a	−0.3545	1	29.01	0.03	0.17	0.59	0.00	0.17	0.00	0.18	0.02	0.11	0.08	1.36
113a	−0.3563	1	28.33	0.12	0.00	3.63	0.01	0.19	0.01	0.29	0.00	0.12	0.08	1.00
112a	−0.3591	1	60.37	0.02	0.09	9.51	0.01	1.04	0.00	0.01	0.00	0.03	0.01	3.37
111a	−0.3711	1	3.29	0.00	0.00	0.40	0.01	0.43	0.00	0.09	0.06	0.23	0.00	0.03
110a	−0.3947	1	2.97	0.04	0.30	1.47	0.01	4.47	0.00	0.02	0.05	0.15	0.00	24.28

[a] Occupation (occ) and MO energies were taken from population analysis. [b] MO coefficients in the natural atomic orbital (NAOMO) analysis.

TABLE 6: Molecular Orbital Descriptions from Population and NAOMO Coefficient Analysis of β-Spin Orbitals of Ni(II)−Az

			Ni(II)[b]		S^{γ}(C112)[b]		$N^{\delta1}$(H46)[b]		$N^{\delta1}$(H117)[b]		S^{δ}(M121)[b]		O(G45)[b]	
orbital level[a]	energy (eV)[a]	occ[a]	3d	4s	3s	3p	2s	2p	2s	2p	3s	3p	2s	2p
122a	−0.1937	0	68.50	0.07	0.08	16.36	0.83	2.74	0.73	2.18	0.00	0.05	0.01	0.20
121a	−0.1959	0	80.65	2.40	0.17	1.69	0.03	0.22	0.21	1.01	0.16	0.59	0.75	2.99
120a	−0.3166	1	13.96	0.30	0.24	62.74	0.00	0.14	0.30	1.35	0.00	5.23	0.02	0.25
119a	−0.3217	1	3.31	0.00	0.02	13.25	0.03	0.20	0.00	0.04	0.00	68.77	0.00	0.04
118a	−0.3244	1	13.18	1.68	0.53	55.87	0.37	1.24	0.11	0.45	0.01	11.25	0.00	0.28
117a	−0.3477	1	0.10	0.00	0.01	0.10	0.00	0.02	0.00	0.00	0.00	0.00	0.00	0.36
116a	−0.3524	1	0.17	0.00	0.02	0.39	0.00	0.09	0.00	0.62	0.03	0.57	0.03	0.41
115a	−0.3529	1	0.67	0.02	0.01	0.58	0.01	0.01	0.02	0.07	0.01	0.02	0.00	1.98
114a	−0.3678	1	0.30	0.01	0.06	0.73	0.00	1.02	0.00	0.02	0.14	0.57	0.00	0.14
113a	−0.3867	1	45.56	0.03	3.67	13.78	0.10	0.50	0.00	7.70	0.01	0.02	0.01	2.70
112a	−0.3912	1	18.40	0.04	0.04	0.79	0.01	0.78	0.00	1.99	0.08	0.25	0.00	23.90
111a	−0.3971	1	54.64	0.05	0.81	2.90	0.05	1.13	0.11	0.49	0.04	0.16	0.45	27.43
110a	−0.4101	1	27.97	0.05	0.08	2.14	0.02	12.15	0.02	0.88	3.24	14.53	0.03	8.55

[a] Occupation (occ) and MO energies were taken from population analysis. [b] MO coefficients in the natural atomic orbital (NAOMO) analysis.

122α and 119β electrons. The 119β is the highest occupied molecular orbital (HOMO) and 120β are the LUMO. The Ni(II)−Az consists of 122α and 120β electrons. The HOMO and LUMO of Ni(II)−Az are 120β and 121β, respectively. Energies of β spin orbitals and its NAOMO compositions obtained from B3LYP/TZVP method for Co(II)−Az and Ni(II)−Az are shown in Tables 5 and 6, respectively.

Atomic Charge and Spin Density. The important electronic properties of the blue copper protein are the distribution of unpaired spin density and charge density. In this context, it is important to mention the previous studies on the calculation of spin density of blue copper protein.[23b] Solomon and co-workers have applied various density functional as well as different population schemes and basis sets to derive the correct trend in the charge and spin density values on the blue copper proteins.[10] Rothlisberger and co-workers have made detailed analysis on the origin of the discrepancy between the calculated and experimental values of charge and spin density of native azurin.[23] They have clearly elicited the importance of electrostatic environment created by the surrounding protein milieu and method of calculation of spin density. It is found that the various density functionals used in the calculation and the choice of population scheme would influence the predicted spin density values.[23b]

The partial charge and spin densities on each atom have been calculated for the active site of native and substituted azurin using MPA and NPA analysis at B3LYP/6-31G*. These results are presented in Tables 7, 8, 9, and 10. The partial charge and total spin density on the metal ion and S^{γ}(C112) depends on their distance. The calculated spin density values for Cu(II) and S^{γ}(C112) are 54.66% and 35.37%, respectively. These results are reasonably closer to the corresponding experimental values of Cu(II) and S^{γ}(C112) atoms, respectively.[23b] This clearly indicates that spin density is strongly delocalized over the Cu(II)−S^{γ}(C112) bond.

The calculated spin density for metal ion and S^{γ}(C112) atoms of Co(II)−Az and Ni(II)−Az are 91.73% for Co(II) and 4.86% for S^{γ}(C112) and 87.77% for Ni(II) and 6.69% for S^{γ}(C112), respectively. In accordance with the decrease in the M(II)−S^{γ}(C112) bond lengths, the spin densities on the metal atoms decrease due to reduction in the M(II)−ligand mixing which vary as Cu(II) > Ni(II) > Co(II). The electron density isosurface of important orbitals of Cu(II)−Az, Co(II)−Az, and Ni(II)−Az are shown in Figure 4. It can be seen that 122β LUMO of Cu(II)−Az has $3d_{x^2-y^2}$ orbital character which interacts with the $3p_{\pi}$ orbital of S^{γ}(C112). Further the $3d_{x^2-y^2}$ orbital overlaps with the $2p_{\sigma}$ orbitals of $N^{\delta1}$(H46) and $N^{\delta1}$(H117). The side views of the isosurface shows the extent of mixing of metal ion and ligand orbitals. The decrease in the overlap of these two orbitals can be found from the electron density isosurface of Co(II)−Az and Ni(II)−Az. The interaction of metal ion $3d_{z^2}$ orbital with axial ligand (S^{δ}(M121) and O(G45)) is evident from the electron density isosurface. The decrease in the overlapping between metal ion and ligand

TABLE 7: Partial Atomic Charges and Total Spin Densities on Each Atom by MPA and NPA for the Cu(II)−Az

		MPA		NPA
residue	atom	atomic charge (a.u.)	atomic spin density (%)	atomic charge (a.u.)
	Cu	0.658351	54.664100	1.282200
C112	C^{β}	−0.583542	−1.643000	−0.789360
	S^{γ}	−0.193890	35.373700	−0.429860
H46	C	0.607892	−0.012600	0.682600
	O	−0.532290	0.088600	−0.642530
	N	−0.587358	0.007200	−0.646310
	C^{α}	−0.058330	−0.102100	−0.124750
	C^{β}	−0.354292	0.082400	−0.498880
	C^{γ}	0.297323	0.176400	0.124380
	$N^{\delta 1}$	−0.583040	3.623700	−0.667680
	$C^{\delta 2}$	0.252594	0.197800	0.220680
	$C^{\varepsilon 1}$	−0.547797	−0.192700	−0.539280
	$N^{\varepsilon 2}$	−0.019184	0.191100	−0.063720
H117	C^{β}	−0.559007	0.087000	−0.722520
	C^{γ}	0.280735	0.182100	0.133640
	$N^{\delta 1}$	−0.585236	4.510200	−0.686950
	$C^{\delta 2}$	0.256101	−0.474600	0.221480
	$C^{\varepsilon 1}$	−0.547171	0.058600	−0.540680
	$N^{\varepsilon 2}$	−0.019576	0.238400	−0.074310
G45	C	0.590916	−0.010500	0.714440
	O	−0.523360	0.010500	−0.705110
	C^{α}	−0.530817	−0.001200	−0.747770
M121	C^{γ}	−0.589815	−0.025400	−0.808770
	S^{δ}	0.063075	−0.023000	0.148500
	C^{ε}	−0.599794	−0.001300	−0.809870
N47	N	−0.605753	0.304100	−0.640020
	C^{α}	−0.320543	0.006500	−0.481570

TABLE 8: Partial Atomic Charges and Total Spin Densities on Each Atom by MPA and NPA for the Co(II)−Az

		MPA		NPA
residue	atom	atomic charge (a.u.)	atomic spin density (%)	atomic charge (a.u.)
	Co	0.872421	91.729600	1.448020
C112	C^{β}	−0.573128	−0.388700	−0.783730
	S^{γ}	−0.337478	4.862633	−0.557630
H46	C	0.618500	−0.054967	0.687530
	O	−0.526034	0.066167	−0.637170
	N	−0.560771	0.144133	−0.612350
	C^{α}	−0.078304	0.180300	−0.141240
	C^{β}	−0.338775	0.009733	−0.495440
	C^{γ}	0.277042	0.058033	0.116740
	$N^{\delta 1}$	−0.601347	0.558667	−0.659070
	$C^{\delta 2}$	0.252163	−0.035667	0.214900
	$C^{\varepsilon 1}$	−0.549594	0.058367	−0.545690
	$N^{\varepsilon 2}$	−0.013899	0.109833	−0.067980
H117	C^{β}	−0.552632	0.024200	−0.721330
	C^{γ}	0.282593	0.094433	0.143030
	$N^{\delta 1}$	−0.594399	0.653833	−0.668800
	$C^{\delta 2}$	0.260229	0.049800	0.208910
	$C^{\varepsilon 1}$	−0.548586	0.082767	−0.543080
	$N^{\varepsilon 2}$	−0.021438	0.041467	−0.077470
G45	C	0.624609	0.046300	0.732220
	O	−0.585773	0.808367	−0.773260
	C^{α}	−0.532891	0.097967	−0.741750
M121	C^{γ}	−0.586986	0.037467	−0.808790
	S^{δ}	0.069106	0.178133	0.155360
	C^{ε}	−0.598068	−0.027900	−0.810760
N47	N	−0.615827	0.100700	−0.648830
	C^{α}	−0.319070	−0.024600	−0.480900

orbitals is in accordance with the calculated charge and spin density values.

Excitation Energy Calculation. Several groups have investigated the spectroscopic properties of blue copper proteins in general and in particular native and substituted azurins.[2−7,10−13,16,20−23] Solomon et al. have used $CuCl_4^{2-}$ as the prototype model system.[10] The spectroscopic data including ground-state spin densities, excitation energies, and their assignments formed the basis for the calibration of various density functionals.[10g] They have used pure generalized gradient approximation (GGA) based Becke exchange and the Perdew−Wang correlation (BP86) functional and hybrid density functionals such as B3LYP and BHandHLYP to study the electronic structure and spectra of blue copper proteins.[10g] In addition, they have evaluated the basis set dependence of these functionals in predicting above-mentioned electronic properties. As mentioned,

TABLE 9: Partial Atomic Charges and Total Spin Densities on Each Atom by MPA and NPA for the Ni(II)-Az

		MPA		NPA
residue	atom	atomic charge (a.u.)	atomic spin density (%)	atomic charge (a.u.)
	Ni	0.815346	87.769850	1.432690
C112	C^{β}	−0.571113	−0.159150	−0.784230
	S^{γ}	−0.297808	6.693750	−0.549760
H46	C	0.615340	−0.009400	0.682750
	O	−0.533149	0.018200	−0.641640
	N	−0.560895	−0.046800	−0.611880
	C^{α}	−0.079687	−0.032250	−0.143750
	C^{β}	−0.346059	0.032500	−0.496690
	C^{γ}	0.279777	0.009250	0.114420
	$N^{\delta 1}$	−0.595372	1.271250	−0.658230
	$C^{\delta 2}$	0.249485	−0.139750	0.213880
	$C^{\varepsilon 1}$	−0.548272	0.044700	−0.541090
	$N^{\varepsilon 2}$	−0.011685	0.132700	−0.062470
H117	C^{β}	−0.564100	0.009300	−0.726740
	C^{γ}	0.278981	0.050650	0.135800
	$N^{\delta 1}$	−0.586874	1.286850	−0.672210
	$C^{\delta 2}$	0.261729	−0.276650	0.213560
	$C^{\varepsilon 1}$	−0.546667	0.030000	−0.541010
	$N^{\varepsilon 2}$	−0.015054	0.150500	−0.071470
G45	C	0.620482	0.016000	0.731430
	O	−0.562319	1.836150	−0.761310
	C^{α}	−0.534591	0.210400	−0.741990
M121	C^{γ}	−0.586922	0.051150	−0.809550
	S^{δ}	0.066958	0.250850	0.156560
	C^{ε}	−0.598720	−0.006750	−0.813550
N47	N	−0.606995	0.091950	−0.639810
	C^{α}	−0.318298	0.002900	−0.480790

TABLE 10: Partial Atomic Charges on Each Atom by MPA and NPA for the Zn(II)−Az

		MPA	NPA
residue	atom	atomic charge (a.u.)	atomic charge (a.u.)
	Zn	0.812088	1.545940
C112	C^{β}	−0.566415	−0.780340
	S^{γ}	−0.317623	−0.600100
H46	C	0.615369	0.683640
	O	−0.534443	−0.643480
	N	−0.566569	−0.615420
	C^{α}	−0.081066	−0.142810
	C^{β}	−0.340749	−0.496030
	C^{γ}	0.277909	0.120450
	$N^{\delta 1}$	−0.589555	−0.690630
	$C^{\delta 2}$	0.252995	0.218110
	$C^{\varepsilon 1}$	−0.545993	−0.539570
	$N^{\varepsilon 2}$	−0.009239	−0.062290
H117	C^{β}	−0.559743	−0.725840
	C^{γ}	0.282450	0.144390
	$N^{\delta 1}$	−0.590002	−0.717500
	$C^{\delta 2}$	0.265668	0.219240
	$C^{\varepsilon 1}$	−0.544172	−0.538160
	$N^{\varepsilon 2}$	−0.016792	−0.071300
G45	C	0.617137	0.735690
	O	−0.565876	−0.791790
	C^{α}	−0.531724	−0.741330
M121	C^{γ}	−0.585246	−0.809350
	S^{δ}	0.059317	0.156190
	C^{ε}	−0.593152	−0.812320
N47	N	−0.607209	−0.640320
	C^{α}	−0.319869	−0.481950

Rothlisberger and co-workers have carried out similar analysis and brought out the importance of protein environment in the prediction of excitation energies.[23]

The ground state of free Cu(II) ion is ^{2}D. Due to the splitting of this free ionic state by the ligand environment, five ligand field (d → d) transitions (LFT) are possible.[16] Free Co(II) ion has a ^{4}F ground state, with a second quartet state ^{4}P lying at 14500 cm^{-1}. Under the influence of a tetrahedral field these levels will split up into $^4A_2$(F), $^4T_2$(F), $^4T_1$(F), and $^4T_1$(P) arranged in order of increasing energy. It is well-known that ten LFT are possible for this system.[16,36] De Kerpel et al. have calculated both LF and LMCT transitions of $Cu(Im)_2(SH)(SH_2)^+$ and $Co(Im)_2(SH)(SH_2)^+(HCONH_2)$ using CASSSCF/CASPT2 approach employing B3LYP geometry.[16] Using these model systems, they have predicted both LF and LMCT transitions of plastocyanin and Co(II)−Az. The ground and first excited states of free Ni(II) ion are ^{3}F and ^{3}P, respectively.[36] Under the influence of a tetrahedral field these levels split into $^3T_1$(F),$^3T_2$(F), $^3T_1$(P), and$^3A_2$(F) arranged in order of increasing energy. Funk et al. have used X-ray magnetic circular dichorism to explore the oxidation states and electronic structure of Ni(II)−Az. In the same study, they have used DFT calculations to analyze the electronic structure of Ni(II)−Az.[37]

Solomon et al.[10] have explained the origin of intense blue transitions in blue copper proteins. It is well-known that electrons are excited from filled d orbitals into half-occupied $3d_{x^2-y^2}$ levels, leading to a weak LFT. The ligand-based orbitals are excited into the half-filled $3d_{x^2-y^2}$ leading to strong LMCT which are more intense when compared to the LFT. Calculated LMCT values at the B3LYP level using different basis sets for native and substituted azurins are listed in Table 11 along with the same reported by others.[2,10g,23b] These values are in good agreement with the experimental excitation energies.[1a] It can be observed from the results that the TDDFT (B3LYP) calculations combined with ONIOM approach reliably predict the excitation energies. It is observed from various studies on the blue copper proteins that the LMCT energy and the intensity of this transition depend on the charge transfer and mixing between $3d_{x^2-y^2}$ orbital of M(II) and $3p_{\pi}$ orbital of S^{γ}(C112).[1,2,10,23b] It can be seen from Tables 4, 5, and 6 that mixing of metal ion 3d orbitals with $3p_{\pi}$ orbital of S^{γ}(C112) decreases as Cu(II) >

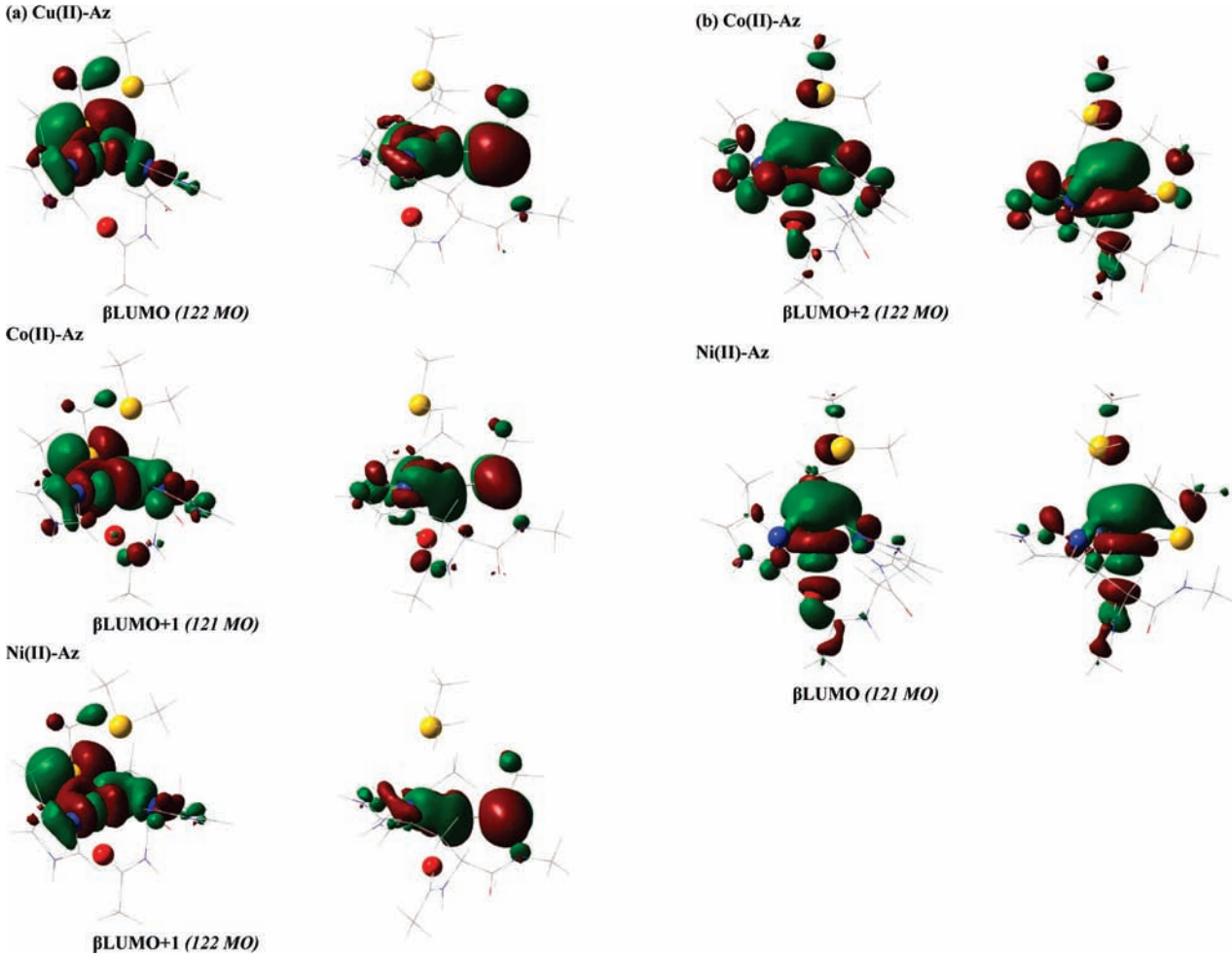

Figure 4. Isodensity surface (isovalue = 0.02 au,) of the empty $3d_\beta$ orbitals: (a) $3d_{x^2-y^2}$ and (b) $3d_{z^2}$ in the active site of Cu(II)−Az, Co(II)−Az, and Ni(II)−Az.

TABLE 11: Calculated Excitation Energies for the Oxidized State of Cu(II)−Az, Co(II)−Az, and Ni(II)−Az Using Various Basis Sets

	calculated excitation energy (nm)					
	6-31G*	6-311G**	TZVP	6-311+G*	6-311+G**	exptl excitation energy (nm)[a]
Cu(II)−Az present study	615	614	642	633	632	629
Solomon et al.[b]			620			
Swart et al.[c]			605			
Rothlisberger et al.[d]			590			
Co(II)−Az present study	322	332	347	349	350	330
Ni(II)−Az present study	447	482	501	505	505	440

[a] Taken from refs 1a, 10g, 2, and 23b. [b] Taken from refs 1a, 10g, 2, and 23b. [c] Taken from refs 1a, 10g, 2, and 23b. [d] Taken from refs 1a, 10g, 2, and 23b.

Ni(II) > Co(II), which is also evident from the electron density isosurface of some important orbitals of native, Ni(II)−Az, and Co(II)−Az.

Further analysis of orbitals provides further insight into the origin of excitation energies. Co(II)−Az and Ni(II)−Az have three ($3d_{x^2-y^2}/3d_{z^2}/3d_{xy}$) and two ($3d_{x^2-y^2}/3d_{z^2}$) holes, respectively, in the high-spin ground state.[16,37] The additional hole in the Co(II)−Az and Ni(II)−Az $3d_\beta$ orbital, $3d_{z^2}$ orbital is more localized than the other orbitals due to the interaction of axial ligands with the $3d_{z^2}$ orbital.[37] It is observed that the pseudo-σ-antibonding interaction of S^γ(C112) with 3*d* orbitals determines the overall composition of the empty $3d_\beta$ orbital. The isosurface presented in Figure 4 clearly exemplifies the charge and spin redistribution in the Co(II)−Az and Ni(II)−Az due to the pseudo-σ (in the $3d_{z^2}$) and π (in the $3d_{x^2-y^2}$) interaction of metal ion d orbital with the p orbital of S^γ(C112).

It has been found from the previous DFT calculations on the model Cu(II)−Az that the equatorial plane of the trigonal site is composed of following interactions involving the metal ion and ligand:[37,10,13,16] (i) the $3d_{x^2-y^2}$ orbital of Cu(II) strongly mixes with sulfur $3p_\pi$ orbital from the equatorial C112 residue. It has a strong π-antibonding interaction between the metal and equatorial ligand (Cu(II)−S^γ(C112)). (ii) the σ-antibonding interaction between the $3d_{x^2-y^2}$ orbital of Cu(II) and $N^{\delta1}$(H46) and $N^{\delta1}$(H117) equatorial residues. These two interactions are modulated by the substitution of metal ion by Co(II)−Az, Ni(II)−Az, and Zn(II)−Az. It is interesting to find that the interaction involved in the stabilization of native and substituted

TABLE 12: Calculated Excitation Energies and Oscillator Strengths of Native and Substituted Azurins

	excitation energy (cm^{-1})[a]			oscillator strength		
no.	Cu(II)−Az	Co(II)−Az	Ni(II)−Az	Cu(II)−Az	Co(II)−Az	Ni(II)−Az
1	6608.86 (1513)	6032.27 (1658)	5709.75 (1751)	0.0002	0.0001	0.0001
2	10826.61 (924)	6834.76 (1463)	6116.88 (1635)	0.0004	0.0001	0.0001
3	14159.89 (706)	7945.15 (1259)	7942.31 (1259)	0.0009	0.0001	0.0002
4	14690.54 (681)	10844.46 (922)	10453.47 (957)	0.0050	0.0010	0.0001
5	15555.49 (642)	13018.29 (768)	14550.75 (687)	0.0010	0.0005	0.0002
6	16881.63 (592)	15142.34 (660)	16471.21 (607)	0.0085	0.0036	0.0015
7	17172.69 (582)	18815.38 (531)	17029.97 (587)	0.0034	0.0026	0.0080
8	17813.88 (561)	21576.84 (463)	19924.68 (501)	0.0011	0.0011	0.0405
9	19120.82 (523)	24731.66 (404)	21287.92 (470)	0.0707	0.0027	0.0152
10	20009.60 (500)	24942.63 (401)	21928.38 (456)	0.0026	0.0005	0.0037
11	20986.36 (477)	25423.94 (393)	24748.19 (404)	0.0002	0.0023	0.0023
12	22415.49 (446)	28120.69 (356)	25143.95 (398)	0.0001	0.0010	0.0024
13	23076.04 (433)	28607.39 (350)	27616.68 (362)	0.0003	0.0222	0.0005
14	31110.00 (321)	28796.87 (347)	28313.37 (353)	0.0002	0.0464	0.0006
15	32209.23 (310)	30068.86 (333)	28373.62 (352)	0.0001	0.0188	0.0002
16	34800.77 (287)	31781.34 (315)	28640.99 (349)	0.0003	0.0004	0.0000
17	34886.97 (287)	32628.56 (306)	29428.21 (340)	0.0000	0.0003	0.0005
18	35056.97 (285)	33377.84 (300)	29753.05 (336)	0.0000	0.0012	0.0017
19	38115.57 (262)	33755.27 (296)	31234.38 (320)	0.0000	0.0007	0.0005
20	38276.05 (261)	33877.63 (295)	31728.91 (315)	0.0021	0.0003	0.0000

[a] Excitation energy (in nm) values are given in parentheses.

azurins are different owing to the splitting of the $3d_\beta$ orbitals. In these substituted systems, the splitting of the $3d_{x^2-y^2}$ and $3d_{xy}$ orbitals are significantly smaller, whereas the $3d_{z^2}$ energy is much higher which is due to the enhanced σ-antibonding character of $3d_{z^2}$.[37] As a result, a shorter M(II)−O(G45) bond is formed. Concomitantly, the decrease in the splitting between $3d_{x^2-y^2}$ and $3d_{xy}$ leads to formation of a longer M(II)−S^γ(C112) bond.[37]

Calculated LF and LMCT transition energies along with the oscillator strength for Cu(II)−Az, Co(II)−Az, and Ni(II)−Az are presented in Table 12. The calculated excitation energies for Cu(II)−Az range from 6608 to 38276 cm^{-1}. With the model system, it has been shown that excitation energies of native azurin which range from 5237 to 15403 cm^{-1} are related to the LF transitions. The two transitions at 15403 and 21506 cm^{-1} are assigned as CT transitions. In the present study, the characteristic CT transition corresponding blue copper proteins occurs at 15555 cm^{-1} (640 nm), which, involves the transition from $117\beta \rightarrow 122\beta$ orbital. The TDDFT calculation provides existence of another possibility of transition from $115\beta \rightarrow 122\beta$. The NAOMO analysis of these orbitals clearly shows the metal ion and ligand characters of 122β and $115\beta/117\beta$ orbitals, respectively, shown in Table 4.

The calculated excitation energies for Co(II)−Az and Ni(II)−Az vary from 6032 to 33877 cm^{-1} and 5709 to 31728 cm^{-1}, respectively. It is found from the earlier calculation on model system that excitation energies in the ranges of 3483−20864 and 25865−33280 cm^{-1} are assigned to LF and CT transitions, respectively. In this study, the transitions from $119\beta \rightarrow 121\beta$, $117\beta \rightarrow 120\beta$, $117\beta \rightarrow 121\beta$, and $117\beta \rightarrow 122\beta$ correspond to the experimental value of 330 nm for the Co(II)−Az. As evident from Table 5, the atomic composition analysis reveals that 119β have the higher ligand character. The LMCT related to experimental value of 440 nm for Ni(II)−Az corresponds to transition from $120\beta \rightarrow 122\beta$ and $118\beta \rightarrow 122\beta$ orbitals. The NAOMO analysis of these orbitals clearly shows 120β orbital has higher ligand nature as depicted in Table 6.

Conclusions

The following important results emerge from the detailed calculations on the native and substituted azurins: (i) The overall protein structure is not modified drastically upon metal ion substitution. However, the metal ion binding site undergoes noticeable changes upon metal ion substitution. (ii) The inclusion of protein environment is necessary to predict the active site geometries of metalloproteins. (iii) The substitution of native Cu(II) by Co(II), Ni(II), and Zn(II) leads to a loss of covalency (M(II)−S^δ(M121)) and concomitantly the ionic interaction (M(II)−O(G45)) increases. (iv) The LMCT transition decreases on metal ion substitution due to the reduction in the overlap of metal ion and ligand orbitals. (v) The calculated geometrical parameters clearly reveal the importance of protein environment in the prediction of structure of the metalloproteins. It is found from the results that ONIOM approach is a powerful strategy to probe the structure and spectra of metalloproteins.

Acknowledgment. This study is supported by the grant from the Department of Science and Technology (DST), Government of India, New Delhi, India, under New Initiatives in Bioinorganic Chemistry. One of the authors (V.S.) wishes to thank Dr. T. Ramasami, for his valuable suggestions and comments.

Supporting Information Available: Geometrical parameters of B3LYP/6-311G** optimized structures. This material is available free of charge via the Internet at http://pubs.acs.org.

References and Notes

(1) (a) Messerschmidt, A.; Huber, R.; Poulos, T.; Wieghardt, K. *Handbook of Metalloproteins*; John Wiley & Sons: New York, 2001. (b) Bertini, I.; Gray, H. B.; Lippard, S. J.; Valentine, J. S. *Bioinorganic Chemistry*; Viva Publications: New Delhi, 2004. (c) Roat-Malone, R. M. *Bioinorganic Chemistry*; John Wiley & Sons: Hoboken, NJ, 2007.

(2) Swart, M. Density functional theory applied to copper proteins. Ph.D. Thesis, Rijkuniversiteit Groningen, Groningen, 2002.

(3) (a) Datta, S. N.; Sudhamsu, J.; Pandey, A. *J. Phys. Chem. B* **2004**, *108*, 8007–8016. (b) Barone, V.; De Rienzo, F.; Langella, E.; Menziani, M. C.; Rega, N.; Sola, M. *Proteins: Struct., Funct., Bioinf.* **2006**, *62*, 262–269. (c) Li, H.; Webb, S. P.; Ivanic, J.; Jensen, J. H. *J. Am. Chem. Soc.* **2004**, *126*, 8010–8019.

(4) (a) Adman, E. T. *Adv. Protein Chem.* **1991**, *42*, 145–149. (b) Ryde, U.; Olsson, M. H. M. *Int. J. Quantum Chem.* **2001**, *81*, 335–347. (c) Lu, Y.; Berry, S. M.; Pfister, T. D. *Chem. Rev.* **2001**, *101*, 3047–3080. (d) van Gastel, M.; Coremans, J. W. A.; Sommerdijk, H.; van Hemert, M. C.; Groenen, E. J. J. *J. Am. Chem. Soc.* **2002**, *124*, 2035–2041.

(5) (a) Lu, Y. *Angew. Chem., Int. Ed.* **2006**, *45*, 5588–5601. (b) Solomon, E. I. *Inorg. Chem.* **2006**, *45*, 8012–8025.

(6) (a) Wilson, M. T.; Greenwood, C.; Brunori, M.; Antonini, E. *Biochem. J.* **1975**, *145*, 449–457. (b) Antonini, E.; Finazzi-Agro, A.; Avigliano, L.; Guerrieri, P.; Rotilio, G.; Mondovi, B. *J. Biol. Chem.* **1970**, *245*, 4847–4856. (c) van de Kamp, M.; Silvestrini, M. C.; Brunori, M.; Beeumen, J. V.; Hali, F. C.; Canters, G. W. *Eur. J. Biochem.* **1990**, *194*, 109–118. (d) Romling, U.; Karen, D.; Schmidt, Tummeler, B. *FEMS Microbiol. Lett.* **1997**, *150*, 149–156. (e) Nelson, D. L.; Cox, M. M. *Lehninger Principles of Biochemistry*; Macmillan Publications: New Delhi, 2000.

(7) (a) Dennison, C. *Coord. Chem. Rev.* **2005**, *249*, 3025–3054. (b) Bizzarri, A. R.; Brunori, E.; Bonanni, B.; Cannistraro, S. *J. Mol. Recognit.* **2007**, *20*, 122–131.

(8) (a) Nar, H.; Messersschmidt, A.; Huber, R.; van de Kamp, M.; Canters, G. W. *J. Mol. Biol.* **1991**, *221*, 765–772. (b) Nar, H.; Messerschmidt, A.; Huber, R.; van de Kamp, M.; Canters, G. W. *FEBS Lett.* **1992**, *306*, 119–24.

(9) (a) Borger, B.; Gutschank, J.; Suter, D.; Thomson, A. J.; Bingham, S. J. *J. Am. Chem. Soc.* **2001**, *123*, 2334–2339. (b) Remenyi, C.; Reviakine, R.; Kaupp, M. *J. Phys. Chem. B* **2007**, *111*, 8290–8304. (c) Sinnecker, S.; Neese, F. *J. Comput. Chem.* **2006**, *27*, 1463–1475.

(10) (a) Penfield, K. W.; Gewirth, A. A.; Solomon, E. I. *J. Am. Chem. Soc.* **1985**, *107*, 4519–4529. (b) Solomon, E. I.; Baldwin, M. J.; Lowery, M. D. *Chem. Rev.* **1992**, *92*, 521–542. (c) Solomon, E. I.; Lowery, M. D. *Science* **1993**, *259*, 1575–1581. (d) Guckert, J. A.; Lowery, M. D.; Solomon, E. I. *J. Am. Chem. Soc.* **1995**, *117*, 2817–2844. (e) Holm, R. H.; Kennepohl, P.; Solomon, E. I. *Chem. Rev.* **1996**, *96*, 2239–2314. (f) Solomon, E. I.; Lever, A. B. P. *Inorganic Electronic Structure and Spectroscopy*; John Wiley & Sons: New York, 1999. (g) Solomon, E. I.; Szilagyi, K. R.; George, S. D.; Basumallick, L. *Chem. Rev.* **2004**, *104*, 419–458. (h) Sarangi, R.; Gorelsky, S. I.; Basumallick, L.; Hwang, H. J.; Pratt, R. C.; Stack, T. D. P.; Lu, Y.; Hodgson, K. O.; Hedman, B.; Solomon, E. I. *J. Am. Chem. Soc.* **2008**, *130*, 3866–3877.

(11) (a) Larsson, S.; Broo, A. *J. Phy. Chem.* **1995**, *99*, 4860–4865. (b) LaCroix, L. B.; Shadle, S. E.; Wang, Y.; Averill, B. A.; Hedman, B.; Hodgson, K. O.; Solomon, E. I. *J. Am. Chem. Soc.* **1996**, *118*, 7755–7768. (c) Pierloot, K.; De Kerpel, J. O. A.; Ryde, U.; Roos, B. O. *J. Am. Chem. Soc.* **1997**, *119*, 218–226. (d) Pierloot, K.; De Kerpel, J. O. A.; Ryde, U.; Olsson, M. H. M.; Roos, B. O. *J. Am. Chem. Soc.* **1998**, *120*, 13156–13166.

(12) (a) Shuku, T.; Sugimori, K.; Sugiyama, A.; Nagao, H.; Sakurai, T.; Nishikawa, K. *Polyhedron* **2005**, *24*, 2665–2670. (b) Sugimori, K.; Shuku, T.; Sugiyama, A.; Nagao, H.; Sakurai, T.; Nishikawa, K. *Polyhedron* **2005**, *24*, 2671–2675. (c) Corni, S.; De Rienzo, F.; Di Felice, R.; Molinari, E. *Int. J. Quantum Chem.* **2005**, *102*, 328–342. (d) Sugiyama, A.; Sugimori, K.; Shuku, T.; Nakamura, T.; Saito, H.; Nagao, H.; Kawabe, H.; Nishikawa, K. *Int. J. Quantum Chem.* **2005**, *105*, 588–595.

(13) (a) Ryde, U.; Olsson, M. H. M. *Int. J. Quantum Chem.* **2001**, *81*, 335–347. (b) Ryde, U.; Olsson, M. H. M.; Roos, B. O.; Borin, A. C. *Theor. Chem. Acc.* **2001**, *105*, 452–462.

(14) (a) Lowery, M. D.; Solomon, E. I. *Inorg. Chim. Acta* **1992**, *198*−*200*, 233–243. (b) van Pouderoyen, G.; Andrew, C. R.; Loehr, T. M.; Sanders-Loehr, J.; Mazumdar, S.; Hill, H. A. O.; Canters, G. W. *Biochemistry* **1996**, *35*, 1397–1407. (c) Chang, S.; Karambelkar, V. V.; Sommer, R. D.; Rheingold, A. L.; Goldberg, D. P. *Inorg. Chem.* **2002**, *41*, 239–248. (d) Chowdhury, A.; Peteanu, L. A. *J. Phys. Chem. B* **2002**, *106*, 3007–3012. (e) Berry, S. M.; Ralle, M.; Low, D. W.; Blackburn, N. J.; Lu, Y. *J. Am. Chem. Soc.* **2003**, *125*, 8760–8768.

(15) (a) Matsunaga, Y.; Fujisawa, K.; Ibi, N.; Miyashita, Y.; Okamoto, K. *Inorg. Chem.* **2005**, *44*, 325–335. (b) Arca, M.; Azimi, G.; Demartin, F.; Devillanova, F. A.; Escriche, L.; Garau, A.; Isaia, F.; Kivekas, R.; Lippolis, V.; Muns, V.; Perra, A.; Shamsipur, M.; Sportelli, L.; Yari, A. *Inorg. Chim. Acta* **2005**, *358*, 2403–2412. (c) Taylor, M. K.; Stevenson, D. E.; Berlouis, L. E. A.; Kennedy, A. R.; Reglinski, J. *J. Inorg. Biochem.* **2006**, *100*, 50–259. (d) Garner, D. K.; Vaughan, M. D.; Hwang, H. J.; Savelieff, M. G.; Berry, S. M.; Honek, J. F.; Lu, Y. *J. Am. Chem. Soc.* **2006**, *128*, 15608–15617.

(16) De Kerpel, J. O. A.; Pierloot, K.; Ryde, U. *J. Phys. Chem. B* **1999**, *103*, 8375–8382.

(17) (a) Nar, H.; Huber, R.; Messerschmidt, A.; Filippou, A. C.; Barth, M.; Jaquinod, M.; van de Kamp, M.; Canters, G. W. *Eur. J. Biochem.* **1992**, *205*, 1123–1129. (b) Moratal, J. M.; Romero, A.; Salgado, J.; Perales-Alargon, A.; Jimenez, H. R. *Eur. J. Biochem.* **1995**, *228*, 653–657. (c) Bonander, N.; Vanngard, T.; Tsai, L. C.; Langer, V.; Nar, H.; Sjolin, L. *Proteins: Struct., Funct., Genet.* **1997**, *27*, 385–394.

(18) (a) Donaire, A.; Salgado, J.; Moratal, J. -M. *Biochemistry* **1998**, *37*, 8659–8673. (b) Czernuszewicz, R. S.; Fraczkiewicz, G.; Zareba, A. A. *Inorg. Chem.* **2005**, *44*, 5745–5752.

(19) (a) Ugurbil, K.; Mitra, S. *Proc. Natl. Acad. Sci. U.S.A.* **1985**, *82*, 2039–2043. (b) Kolczak, U.; Salgado, J.; Siegal, G.; Saraste, M.; Canters, G. W. *Biospectroscopy* **1999**, *5*, S19–S32.

(20) (a) Tennent, D. L.; McMillin, D. R. *J. Am. Chem. Soc.* **1979**, *101*, 2307–2311. (b) Di Bilio, A. J.; Chang, T. K.; Malmstrom, B. G.; Gray, H. B.; Karlsson, B. G.; Nordling, M.; Pascher, T.; Lundberg, L. G. *Inorg. Chim. Acta* **1992**, *198*−*200*, 145–148. (c) Cimei, T.; Bizzarri, A. R.; Cannistraro, S.; Cerullo, G.; De Silvestri, S. *Chem. Phys. Lett.* **2002**, *362*, 497–503.

(21) van den Bosch, M.; Swart, M.; Snijdersdagger, J. G.; Berendsen, H. J. C.; Mark, A. E.; Oostenbrink, C.; van Gunsteren, W. F.; Canters, G. W. *ChemBioChem* **2005**, *6*, 738–746.

(22) Runge, E.; Gross, E. K. U. *Phys. Rev. Lett.* **1984**, *52*, 997–1000.

(23) (a) Cascella, M.; Magistrato, A.; Tavernelli, I.; Carloni, P.; Rothlisberger, U. *Proc. Natl. Acad. Sci. U.S.A.* **2006**, *103*, 19641–19646. (b) Cascella, M.; Cuendet, M. A.; Tavernelli, I.; Rothlisberger, U. *J. Phys. Chem. B* **2007**, *111*, 10248–10252.

(24) (a) Siegbahn, P. E. M.; Blomberg, M. R. A. *Chem. Rev.* **2000**, *100*, 421–437. (b) Siegbahn, P. E. M. *J. Comput. Chem.* **2001**, *22*, 1634–1645. (c) Blomberg, M. R. A.; Siegbahn, P. E. M. *J. Phys. Chem. B* **2001**, *105*, 9375–9386. (d) Pelmenschikov, V.; Blomberg, M. R. A.; Siegbahn, P. E. M. *J. Biol. Inorg. Chem.* **2002**, *7*, 284–298. (e) Pelmenschikov, V.; Siegbahn, P. E. M. *Inorg. Chem.* **2002**, *41*, 5659–5666. (f) Siegbahn, P. E. M. *Q. Rev. Biophys.* **2003**, *36*, 91–145. (g) Prabhakar, R.; Siegbahn, P. E. M. *J. Am. Chem. Soc.* **2004**, *126*, 3996–4006. (h) Siegbahn, P. E. M. *Adv. Inorg. Chem.* **2004**, *56*, 101–125. (i) Bassan, A.; Blomberg, M. R. A.; Siegbahn, P. E. M.; Que, L., Jr. *Angew. Chem.* **2005**, *44*, 2939–2941. (j) Siegbahn, P. E. M.; Borowski, T. *Acc. Chem. Res.* **2006**, *39*, 729–738. (k) Blomberg, M. R. A.; Johansson, A. J.; Siegbahn, P. E. M. *Inorg. Chem.* **2007**, *46*, 7992–7997. (l) Siegbahn, P. E. M. *Inorg. Chem.* **2008**, *47*, 1779–1786.

(25) (a) Dapprich, S.; Komaromi, I.; Byun, K. S.; Morokuma, K.; Frisch, M. J. *J. Mol. Struct. (THEOCHEM)* **1999**, *461*−*462*, 1–21. (b) Tschumper, G. S.; Morokuma, K. *J. Mol. Struct. (THEOCHEM)* **2002**, *592*, 137–147. (c) Torrent, M.; Vreven, T.; Musaev, D. G.; Morokuma, K.; Farkas, O.; Schlegel, H. B. *J. Am. Chem. Soc.* **2002**, *124*, 192–193. (d) Pelmenschikov, V.; Siegbahn, P. E. M. *Inorg. Chem.* **2002**, *41*, 5659–5666. (e) Vreven, T.; Morokuma, K. *Theor. Chem. Acc.* **2003**, *109*, 125–132. (f) Morokuma, K. *Bull. Korean Chem. Soc.* **2003**, *24*, 797–801.

(26) (a) Li, J.; Cross, J. B.; Vreven, T.; Meroueh, S. O.; Mobashery, S.; Schlegel, H. B. *Proteins* **2005**, *61*, 246–257. (b) Prabhakar, R.; Vreven, T.; Morokuma, K.; Musaev, D. G. *Biochemistry* **2005**, *44*, 11864–11871. (c) Vreven, T.; Frisch, M. J.; Kudin, K. N.; Schlegel, H. B.; Morokuma, K. *Mol. Phys.* **2006**, *104*, 701–714. (d) Vreven, T.; Byun, K. S.; Komaromi, I.; Dapprich, S.; Montgomery, J. A., Jr.; Morokuma, K.; Frisch, M. J. *J. Chem. Theory Comput.* **2006**, *2*, 815–826. (e) Lundberg, M.; Morokuma, K. *J. Phys. Chem. B* **2007**, *111*, 9380–9389.

(27) Becke, A. D. *J. Chem. Phys.* **1993**, *98*, 5648–5652.

(28) Lee, C.; Yang, W.; Parr, R. G. *Phys. Rev. B* **1988**, *37*, 785–789.

(29) Rappe, A. K.; Casewit, C. J.; Colwell, K. S.; Goddard, W. A., III; Skiff, W. M. *J. Am. Chem. Soc.* **1992**, *114*, 10024–10035.

(30) Hehre, W. J.; Radom, L.; Schleyer, P. V. R.; Pople, J. A. *Ab Initio Molecular Orbital Theory*; Wiley-Interscience: New York, 1986.

(31) (a) Mulliken, R. S. *J. Chem. Phys.* **1955**, *23*, 1833. (b) Reed, A. E.; Weinhold, F. *J. Chem. Phys.* **1983**, *78*, 4066–4073. (c) Reed, A. E.; Weinstock, R. B.; Weinhold, F. *J. Chem. Phys.* **1985**, *83*, 735–746.

(32) Frisch, M. J.; Trucks, G. W.; Schlegel, H. B.; Scuseria, G. E.; Robb, M. A.; Cheeseman, J. R.; Montgomery, J. A., Jr.; Vreven, T.; Kudin, K. N.; Burant, J. C.; Millam, J. M.; Iyengar, S. S.; Tomasi, J.; Barone, V.; Mennucci, B.; Cossi, M.; Scalmani, G.; Rega, N.; Petersson, G. A.; Nakatsuji, H.; Hada, M.; Ehara, M.; Toyota, K.; Fukuda, R.; Hasegawa, J.; Ishida, M.; Nakajima, T.; Honda, Y.; Kitao, O.; Nakai, H.; Klene, M.; Li, X.; Knox, J. E.; Hratchian, H. P.; Cross, J. B.; Bakken, V.; Adamo, C.; Jaramillo, J.; Gomperts, R.; Stratmann, R. E.; Yazyev, O.; Austin, A. J.; Cammi, R.; Pomelli, C.; Ochterski, J. W.; Ayala, P. Y.; Morokuma, K.; Voth, G. A.; Salvador, P.; Dannenberg, J. J.; Zakrzewski, V. G.; Dapprich, S.; Daniels, A. D.; Strain, M. C.; Farkas, O.; Malick, D. K.; Rabuck, A. D.; Raghavachari, K.; Foresman, J. B.; Ortiz, J. V.; Cui, Q.; Baboul, A. G.; Clifford, S.; Cioslowski, J.; Stefanov, B. B.; Liu, G.; Liashenko, A.; Piskorz, P.; Komaromi, I.; Martin, R. L.; Fox, D. J.; Keith, T.; Al-Laham, M. A.; Peng, C. Y.; Nanayakkara, A.; Challacombe, M.; Gill, P. M. W.; Johnson, B.; Chen, W.; Wong, M. W.; Gonzalez, C.; Pople, J. A. *Gaussian 03, revision E.01*; Gaussian, Inc.: Wallingford, CT, 2004.

(33) (a) Jimenez, H. R.; Salgado, J.; Moratal, J. M.; Badarau, I. M. *Inorg. Chem.* **1996**, *35*, 2737–2741. (b) Goodman, D. C.; Reibenspies, J. H.; Goswami, N.; Jurisson, S.; Darensbourg, M. Y. *J. Am. Chem. Soc.* **1997**, *119*, 4955–4963. (c) Henson, N. J.; Hay, P. J.; Redondo, A. *Inorg. Chem.* **1999**, *38*, 1618–1626. (d) Baffert, C.; Artero, V.; Fontecave, M. *Inorg. Chem.* **2007**, *46*, 1817–1824. (e) Barbaro, P.; Bianchini, C.; Giambastiani, G.; Rios, I. G.; Meli, A.; Oberhauser, W.; Segarra, A. M.; Sorace, L.; Toti, A. *Organometallics* **2007**, *26*, 4639–4651. (f) Buchalski, P.; Grabowska, I.; Karaskiewicz, A.; Suwinska, K.; Jerzykiewicz, L. *Organometallics* **2008**, *27*, 3316–3319. (g) Carabineiro, S. A.; Bellabarba, R. M.; Gomes, P. T.; Pascu, S. I.; Veiros, L. F.; Freire, C.; Pereira, L. C. J.; Henriques, R. T.; Oliveira, M. C. O.; Warren, J. E. *Inorg. Chem.* **2008**, *47*, 8896–8911.

(34) (a) Zilbermann, I.; Maimon, E.; Cohen, H.; Meyerstein, D. *Chem. Rev.* **2005**, *105*, 2609–2626. (b) Liu, C. S.; Wang, J. J.; Yan, L. F.; Chang, Z.; Bu, X. H.; Sañudo, E. C; Ribas, J. *Inorg. Chem.* **2007**, *46*, 6299–6310. (c) Desrochers, P. J.; Duong, D. S.; Marshall, A. S.; Lelievre, S. A.; Hong,

B.; Brown, J. R.; Tarkka, R. M.; Manion, J. M.; Holman, G.; Merkert, J. W.; Vicic, D. A. *Inorg. Chem.* **2007**, *46*, 9221–9233. (d) Stevenson, S.; Chancellor, C. J.; Lee, H. M.; Olmstead, M. M.; Balch, A. L. *Inorg. Chem.* **2008**, *47*, 1420–1427. (e) Li, J.; Song, H.; Cui, C.; Cheng, J. P. *Inorg. Chem.* **2008**, *47*, 3468–3470. (f) Habib, M.; Karmakar, T. K.; Arom, G.; Ribas-Ari, J.; Fun, H. K.; Chantraprommaa, S.; Chandra, S. K. *Inorg. Chem.* **2008**, *47*, 4109–4117. (g) Desrochers, P. J.; Corken, A. L.; Tarkka, R. M.; Besel, B. M.; Mangum, E. E.; Linz, T. N. *Inorg. Chem.* **2009**, *48*, 3535–3541.

(35) (a) Wyrwa, R.; Frohlich, H. O.; Gorls, H. *Organometallics* **1996**, *15*, 2833–2835. (b) Darensbourg, D. J.; Wildeson, J. R.; Yarbrough, J. C. *Organometallics* **2001**, *20*, 4413–4417. (c) Aoki, S.; Kimura, E. *Chem. Rev.* **2004**, *104*, 769–788. (d) Gupta, S. P. *Chem. Rev.* **2007**, *107*, 3042–3087. (e) Chai, Z. Y.; Zhang, C.; Wang, Z. X. *Organometallics* **2008**, *27*, 1626–1633. (f) Javed, S.; Hoffman, D. M. *Inorg. Chem.* **2008**, *47*, 11984–11992. (g) Labourdette, G.; Lee, D. J.; Patrick, B. O.; Ezhova, M. B.; Mehrkhodavandi, P. *Organometallics* **2009**, *28*, 1309–1319.

(36) Ballhausen, C. J. *Introduction to Ligand Field Theory*; McGraw-Hill: New York, 1962.

(37) Funk, T.; Kennepohl, P.; Di Bilio, A. J.; Wehbi, W. A.; Young, A. T.; Friedrich, S.; Arenholz, E.; Gray, H. B.; Cramer, S. P. *J. Am. Chem. Soc.* **2004**, *126*, 5859–5866.

JP900451F